Measurements of Electron Velocity Distribution Function (invited paper)

C. Sozzi, E. De La Luna, D. Farina, J. Fessey, L. Figini et al.

Citation: AIP Conf. Proc. **988**, 73 (2008); doi: 10.1063/1.2905123
View online: http://dx.doi.org/10.1063/1.2905123
View Table of Contents: http://proceedings.aip.org/dbt/dbt.jsp?KEY=APCPCS&Volume=988&Issue=1
Published by the American Institute of Physics.

Measurements of Electron Velocity Distribution Function (invited paper)

C.Sozzi[1], E. De La Luna[2], D.Farina[1], J.Fessey[3], L.Figini[1], S.Garavaglia[1], G.Grossetti[1], S.Nowak[1], P.Platania[1], A.Simonetto[1], M.Zerbini[4], and JET EFDA contributors[*]

JET-EFDA, Culham Science Centre, OX14 3DB, Abingdon, UK

[1]*IFP-CNR, Associazione EURATOM-ENEA-CNR sulla Fusione,Via R.Cozzi 53, 20152 Milano ITALY*

[2]*Asociación EURATOM-CIEMAT, CIEMAT, Av.Complutense 22, 28040 Madrid, Spain*

[3]*EURATOM-UKAEA Fusion Association, Culham Science Centre, Abingdon, Oxon, OX14 3DB, UK*

[4]*Associazione EURATOM-ENEA sulla Fusione,C.R.E. Via Enrico Fermi 45 00044 Frascati (Roma), Italy*

Abstract. Deviations of the electron function velocity distribution from Maxwellian behavior in the high energy range have been extensively studied during the past two decades. A brief review of the experimental techniques and findings on the subject is given in this paper. There are indications that the electron distribution function in thermonuclear plasmas could be significantly different from the Maxwellian one even near the thermal velocity range when particular circumstances occur. These reasons motivate a renewed effort in the measurements that could detect low energies distortions, among which is the new Oblique Electron Cyclotron Emission diagnostics that has entered operations during 2006 experimental campaign at JET and aims to resolve relatively small differences in the ECE spectra taken at three toroidal angles. Such measurements allow insight into the characteristics of the electron distribution function. First results of such experimental system are discussed in this paper, along with emission simulations.

Keywords: Electron velocity distribution, Oblique Electron Cyclotron Emission.
PACS: 52.25.Tx, 52.70.Gw, 52.70.La

INTRODUCTION

There are several physics situation in which the features of the electron distribution function (edf) can play a role in modern devices for plasma magnetic confinement, and there have been in fact several experiments in which this characterization has been performed. The edf can depart from the canonical Maxwellian when intense electron heating and/or current drive techniques are applied [1,2], in presence of intense electric field at low plasma density [3], in disruptions and in magnetic reconnections related with magnetohydrodynamic activity [4,5]. It is well known that in such situations high energy tails in the function distribution can develop, producing characteristic signatures in the Electron Cyclotron Emission and in the X-rays Bremmstralung radiation.

[*] See the App. of M.L.Watkins et al., Proc. 21st IAEA Int. Fusion Energy Conference, Chengdu, China (2006)

CP988, *Burning Plasma Diagnostics*, edited by F. P. Orsitto, G. Gorini, E. Sindoni, and M. Tardocchi
2008 American Institute of Physics 978-0-7354-0507-3/08/$23.00

A more elusive phenomenon is the deformation of the electron distribution in the low energy (thermal) range. A few experimental evidences and extensive simulation work [6-8] indicate that the bulk of the electron population itself could be diverted, under particular situations, from the standard maxwellian behavior. If confirmed these observations imply a major rethinking of what concerns the electron kinetic measurements and their interpretation, such the impossibility in principle to give the definition of the temperature as a scalar plasma parameter.

In this paper a brief overview of the experimental techniques used to characterize the electron velocity distribution is given, along with the major findings of such experiments, followed by a description of the work that is being carried out at JET on the subject of the characterization of edf in the thermal energy range.

EDF STUDIES IN THE SUPERTHERMAL ENERGY RANGE

Most of the techniques for the characterization of the edf in the superthermal energy range were originally developed in connection with studies related with Lower Hybrid Current Drive. Such experiments demonstrated the formation of a pronounced, non isotropic fast electrons tail in the distribution function when LHCD is applied, which effectively sustains the plasma current with reduced or even absent inductive electric field [9-14]. More recently, with the development of high power sources in the range of frequency of the Electron Cyclotron resonances in modern toroidal devices, the perspective of a fine control of the current profile has been disclosed, based on the high localization of the EC absorption when compared with the LH one. Effects related with the absorption by superthermal electrons have been observed in ECRH/ECCD experiments, both when the superthermal fraction is generated by EC Resonance Heating and/or Current Drive itself, and when the ECRH/ECCD waves interact with the fast electron tail generated by other means [2]. The experimental techniques used to study the formation and relaxation dynamics of the tails and the absorption properties of fast electrons include soft and hard X emission [14, 15], EC Emission and EC Transmission in various geometrical arrangements [9-13,16]. A general problem with the measurements related to the edf is that a unique reconstruction of the edf itself is not possible without a priori assumption, and the measurements only supply constraints for the actual distribution [17]. Important pieces of information can be inferred by the comparison of different lines of sight of the ECE spectrum, particularly in the cases in which the propagation of the superthermal emission is not hided behind the thermal emission layer. The spatial resolution of the ECE diagnostics is rooted in the physical process of emission-reabsorption of the resonant electrons in a given spatial location and is the result of the interplay among the plasma kinetic parameters (density and temperature), the angle of propagation with respect to the magnetic field and the existence of multi-harmonics resonances and cut-off layers. X-rays based diagnostics instead can be arranged with high number of chords to produce tomography reconstruction with accurate spatial resolution. Table 1 summarizes typical diagnostic figures for the measurement techniques used in electron heating experiments or edf-related studies in toroidal devices. The figures here reported reflect the specific experimental conditions and do not represent absolute limits. Use of oblique ECE and Thomson Scattering in the thermal energy range will be discussed in the next section.

Table 1. Diagnostics for electron distribution measurements

Diagnostics	Energy range	Energy resolution	Spatial localization	Time resolution	Typical application
Soft X [15]	1-20 KeV	10%-20%	r/a~0.1 or less with tomography	~0.01ms	MHD events, Runaway el.
Hard X [14]	20KeV-1MeV	10%-20%	r/a~0.1 or less with tomography	1-10ms	Energetic runaway, LHCD tails,
Vertical ECE [10, 11]	30-250 KeV	15%	chord integrated	~10ms	Runaway, LHCD tails
Vertical microwave transm. [12]	50-200 KeV	10%	chord integrated	5ms	Relativistic EC absorption, LHCD tails
Oblique microwave transm. [9]	1-100 KeV depending on angle	10%-20%	chord integrated	1-5ms	LHCD tails
Oblique ECE [13]	0.1-200 KeV depending on angle	5%	depending on optical thickness and angle	~1ms	LHCD tails, bulk electrons, ECRH
HFS ECE [16]	10-50 KeV	~10%	r/a~0.04-0.25 depending on optical thickness	~0.01ms	ECCD tail, ECRH
Thomson Scatt. [18]	0.1-30 KeV	20%	r/a~0.1 or less	~0.05s	Bulk electrons

EDF STUDIES IN THE THERMAL ENERGY RANGE

Much less effort has been dedicated so far to the detailed study of the edf in the thermal energy range. Besides the question of principle, it has a direct impact on the value ascribed to the electron temperature, being the last essentially the perpendicular slope of the edf. Among the diagnostics listed in table 1, in principle both Oblique ECE (ObECE) and Thomson Scattering (TS) appear to be suitable to investigate this subject. In the TS diagnostics the spectral density function $S(\omega_s)$ of the light scattered by the electrons in the plasma is related with the velocity distribution of the electron population:

$$S(\omega_s, \vartheta, \vec{x}) = F\left[f(\vec{v}, \vec{x})\right] \tag{1}$$

where ω_s is the scattered angular frequency, θ is the scattering angle, $\vec{v}$ and $\vec{x}$ are the velocity and space vectors, F represents an integration operator in the normalized velocity space v/c, and f is the edf. The relation from S and f is then rather direct. In most of present diagnostic systems the scattered light is collected using a finite (sometime small) number of spectral channels and S interpreted assuming f as a Maxwellian. Provided that an adequate number of spectral channels are available and that a sufficient photon statistics is gathered significant deviations from Maxwellian should be detected [17].

A peculiar characteristic of the EC physics is that only resonant electron in a given position in real space and in momentum space contribute to the emission or absorption of EC waves. Being the resonance condition

$$\omega - k_{//} v_{//} = \frac{m\Omega_{ce}}{\gamma} \tag{2}$$

where $n_{//}=ck_{//}/\omega$ is the parallel (to the magnetic field) index of refraction, m the harmonics number, $\Omega_{ce}=eB/mc$ is the resonance frequency and $\gamma=1/(1-v^2/c^2)^{1/2}$ is the relativistic factor, when ECE radiation is observed at an angle significantly different from perpendicular ($n_{//} \neq 0$), a Doppler shift is included in the resonance condition and a range of electron energies can contribute to the emission at a given frequency [18, 19]. The situation is described in figure 1, where a Maxwellian distribution (contour plots electron density in velocity space, in grayscale) is superimposed to a family of resonance curves (dashed lines with increasing $m\Omega_{ce}/\omega$). For perpendicular propagation (left) each resonant curve is close to a single electron energy. For oblique propagation (right) each resonance curve cross a wider range of electron energies, asymmetric with respect to the parallel velocity. Then, diagnosing different harmonics and lines of sight different regions of the electron population momentum space are sampled, and from the merging of those data details of the distribution function can be inferred.

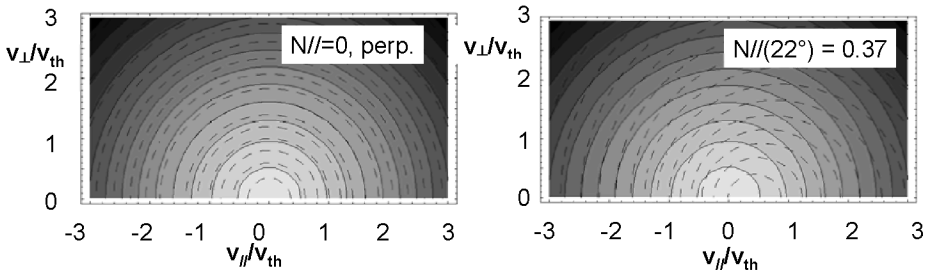

Figure 1. Contours of $f(v_e)$ for a Maxwellian distribution, on which the resonance curves for perpendicular (left) and oblique (right) are superimposed. Grey levels: electron density in velocity space. Dashed lines: resonance curves with increasing $m\Omega_{ce}/\omega$.

Experimental observations having reference to thermal energy range distortions of edf have been observed in TFTR [6], FTU [7] and JET [8] through discrepancies between the electron temperature measured with ECE and Thomson scattering in the plasma core, and through discrepancies between 2nd and 3rd harmonics ECE temperature peaks in optically thick plasmas or other anomalies noticed in the ECE spectrum. Moreover, the first Oblique ECE measurements performed on FTU under intense EC heating showed a discrepancy between perpendicular and oblique ECE measurements indicating again low energy non Maxwellian edf. Common features of the experimental situations in which such observations were performed are high electron temperature, high power heating and low plasma density. However, no extensive experimental studies pointing out detailed cause-effect relations have been performed yet.

OBLIQUE ECE AT JET

The Oblique ECE system of JET has been proposed mainly to perform systematic studies of edf in the thermal energy range, namely to resolve small deviations from Maxwellian-related ECE spectra taken at different toroidal angles. The practical opportunity came with the installation of the so called Microwave Access which includes six circular waveguides, 4 of which corrugated dedicated to Reflectometry diagnostics and 2 smooth dedicated to the oblique lines of sight for ECE. The Oblique ECE system (see figure 2) has three lines of sight respectively at 0° (X polarization only), ~10°, ~22° with respect to the perpendicular to the toroidal magnetic field. The antenna for the oblique lines are built in a single piece, with minimum overall dimensions. The perpendicular sight is positioned in a different octant of the vessel, also equipped with two other ECE diagnostics, a 96 channels radiometer and a perpendicular view Michelson interferometer. Each one of the two quasi optical oblique antennas collect ECE radiation along two linear polarizations (vertical and horizontal) corresponding respectively to mainly X and mainly O polarizations.

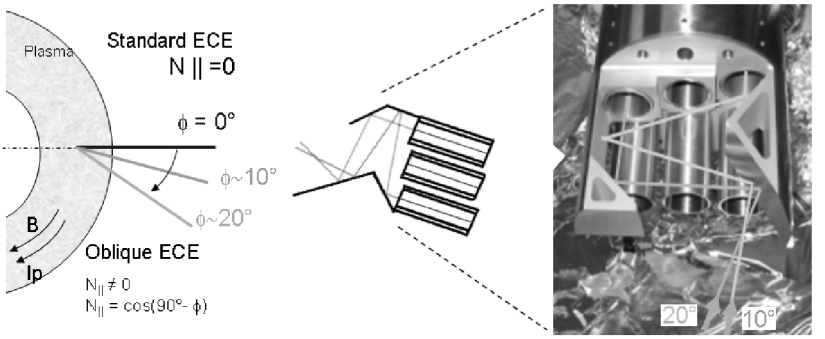

Figure 2. Left: lines of sight of Oblique ECE diagnostics with respect to plasma current and toroidal magnetic field. Centre: sketch of the quasi optical antennae (top view). Right: antenna block before installation in the vessel.

The spectral analysis is performed with a six channel Martin Puplett interferometer (one channel is presently unused), 75-800 GHz band, 7.5-15 GHz single line equivalent spectral resolution [20], being ~350 GHz the maximum frequency of interest for JET. A peculiar feature of the system is that the moving arm of all the channels is realized with a single helix-shaped mirror composed by four sectors. Rapid spinning on the helix (up to 2500 rpm in present configuration) allows time resolution up to 6 ms per radial profile. Due to oblique propagation, the polarization seen by the oblique antennas is elliptical, that is a combination of the pure O and X modes. The amount of "mode contamination", i.e. the fraction of X-mode coupled to the "vertical" polarization of the antenna, increases with the frequency varying from 96% (75 GHz) to 75% (350 GHz) at 10° and from 85% (75 GHz) to 60% (350 GHz) at 22°.

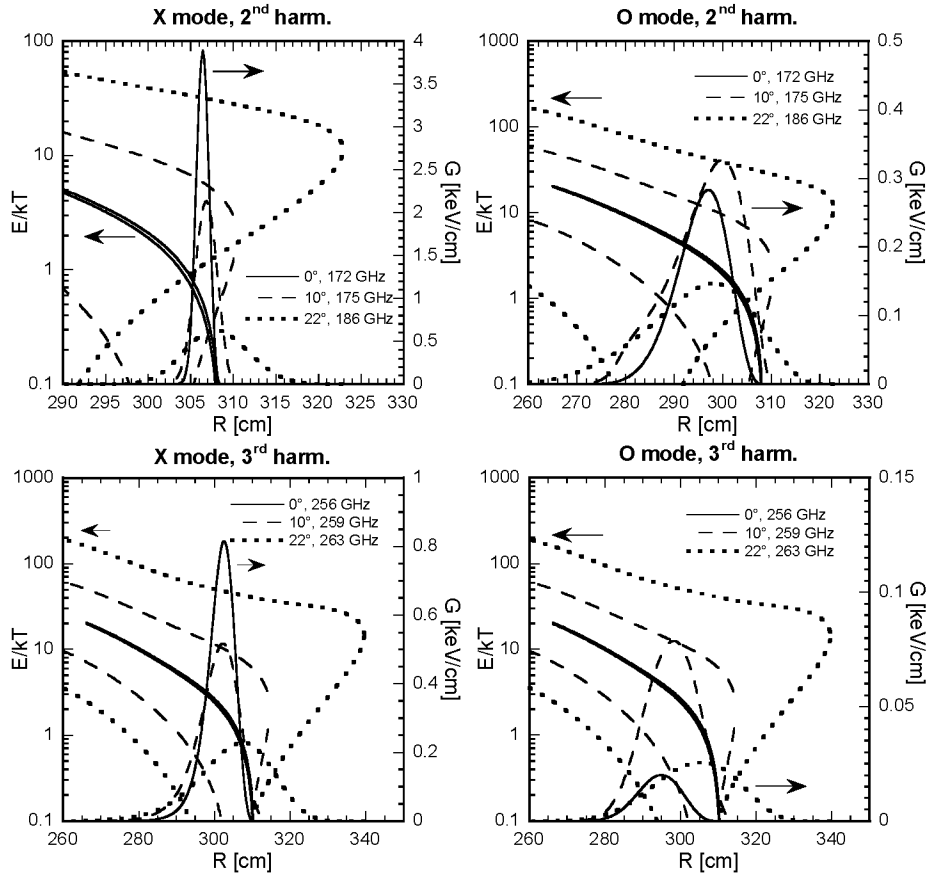

Figure 3. Energy of the emitting electrons (left axis of each plot) normalized to the electron temperature and line width G of the emission (right axis).

Plots in figure 3 show calculations performed with the code SPECE [21] for the shot 68394 (B_T=3.2T, I_p=2.3MA, $n_e d$/=9.1 10^{19}m^{-2}, 16MW NBI + 8MW ICRF). The line width $G = \alpha T_e e^{-\tau}$ of the ECE emission, where α is the absorption coefficient and τ the optical depth is plotted against the left hand y scale. Minimum and maximum branches of the resonance energy of the electron population contributing to a given spectral frequency are instead plotted against the right hand scale. Curves in figure 3 are plotted for the three frequencies respectively corresponding to the peak emission of 2nd and 3rd harmonic, X and O polarizations, at the three angle of sight of the Oblique ECE diagnostics. Calculations are done assuming purely Maxwellian energy distribution for the electrons. Examination of the energy curves for the different cases shows that for increasing angles of emission the energy of contributing electrons increases both in value and in range extension. In particular, perpendicular propagation corresponds to nearly monoenergetic electron population (in a given spatial location) in

the thermal range for X polarization, 2nd harmonic or slightly higher in the other cases. The line width of emission tends to increase with the angle as well.

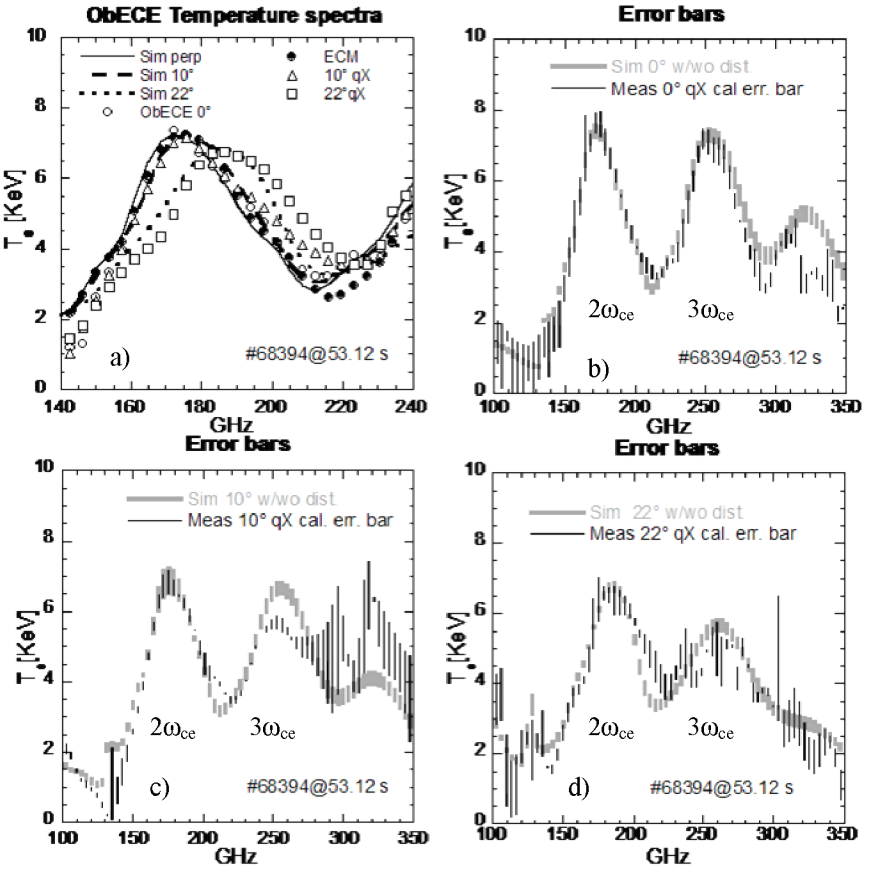

Figure 4. Top left: quasi X-mode, 2nd harmonic perpendicular and oblique measurements of the temperature spectra compared with Maxwellian simulation for the second harmonic peak. Other plots: temperature spectra with error bars due to the calibration procedure compared with simulated spectra for which a small fraction of non maxwellian population is assumed (see text).

In figure 4 the measured quasi X-mode temperature spectra for JET shot 68394 are shown. Spectra in a) show the expected shift in frequency of the peak of emission with angle. Decreasing height of the peak with angle is mainly related with the increasing O fraction, characterized by minor optical depth, reaching the antenna with vertical polarization. The other plots in figure 4 show the measured spectra with the uncertainty introduced by typical calibration errors compared with simulations in which different assumptions on the electron edf are taken. The error bars in the simulated spectra represent the expected variation in the emission if a small fraction of non-maxwellian electrons in the thermal energy range is switched on/off. The distortion here considered has parameters $u_d=\pm 1.2$, $T_d=0.23$, $n_d=0.015$, where u_d is the location of the distortion in velocity space, T_d is the temperature and n_d is the fraction of electrons involved. This

particular distortion is not necessarily the most probable, however it sets a reference value with respect to the diagnostics sensitivity. Work to reduce the error bar of the measurements and to extend the frequency range with reliable calibration is in progress.

CONCLUSIONS

A brief review of the motivations, techniques and results of the experimental studies on the electron function distribution has been given. The field is being revisited on sight of burning plasmas scenario with special attention to possible effects in the thermal energy range. Compact antenna design and well established theoretical basis enable Oblique ECE as an effective techniques for these studies. A dedicated Oblique ECE system has been installed at JET and first results have been discussed. Feasibility studies of oblique lines of sight in ITER based on JET design are being considered and reported elsewhere [21].

ACKNOWLEDGMENTS

A complete overview of the current and past activities in the field is beyond the scope of this paper. The authors apologize for unintended omissions. The work leading to this article was funded by the European Atomic Energy Community and is subject to the provisions of the European Fusion Development Agreement (EFDA Task Agreement JW2-TA-EP-MWA-036).

REFERENCES

1. S. Bernabei et al., Phys. Rev. Lett. **49**, (1982) 1255
2. S. Coda et al., PPCF **48**, (2006) B359-B369 and references therein
3. V.S. Vlasenkov et al., Nucl. Fusion **13**, (1973), 509
4. V. V. Plyusnin et al., Nucl. Fusion **46**, (2006) 277
5. P. V.Savrukhin, Phys. Rev. Lett. **86**, (2001) 3036
6. G Taylor et al., PPCF **36**, (1994), 523
7. O. Tudisco et al., 28th EPS conf. on Contr. Fusion Plasma Phys., Funchal, Pt,. ECA **25A** (2001) 1221
8. E. de la Luna et al., Rev. Sci. Instr. **74**, (2003) 1414 and V. Krivenski, Fus. Eng. Des. **53**, (2001) 23
9. F. Skiff et al., PPCF **36**, (1994) 1371
10. T.C. Luce at al., Rev. Sci. Instr. **59**, (1988) 1593
11. K. Kato and I.H. Hutchinson, Phys. Fluids **30**, (1987), 3809
12. J. L. Ségui and G. Giruzzi, PPCF **36** (1994) 897-910 and references therein.
13. S. Preische et al., Phys. Plasmas **3** (1996) 4065
14. Y. Peysson et al., Nucl. Instr. Methods **A 458** (2001) 269
15. L.C. Ingesson et al., Nucl. Fusion **38**, (1988) 1675
16. P.Blanchard at al, PPCF **44** (2002), 2231 and JFM van Gelder PPCF **40**, (1998) 1185
17. G.Zhuang et al., PPCF **47**, (2005) 1539
18. U. Gasparino, **EC-8** Proc. of 8th Joint workshop on ECE and ECRH, Gut Ising, Germany, (1992) 19
19. E. de la Luna, this Proceedings
20. S. Garavaglia, A. Simonetto, C. Sozzi et al., Fus. Eng. Des. **82**, (2007) 5
21. D. Farina, L. Figini, P. Platania and C. Sozzi, this Proceedings